

K⁺ transport and capacitance of the basolateral membrane of the larval frog skin

Stanley D. Hillyard, Horacio F. Cantiello and Willy Van Driessche
Am J Physiol Cell Physiol 273:1995-2001, 1997.

You might find this additional information useful...

This article cites 24 articles, 15 of which you can access free at:

<http://ajpcell.physiology.org/cgi/content/full/273/6/C1995#BIBL>

This article has been cited by 1 other HighWire hosted article:

Interrelations/cross talk between transcellular transport function and paracellular tight junctional properties in lung epithelial and endothelial barriers

W. Van Driessche, J. L. Kreindler, A. B. Malik, S. Margulies, S. A. Lewis and K.-J. Kim
Am J Physiol Lung Cell Mol Physiol, September 1, 2007; 293 (3): L520-L524.

[\[Abstract\]](#) [\[Full Text\]](#) [\[PDF\]](#)

Medline items on this article's topics can be found at <http://highwire.stanford.edu/lists/artbytopic.dtl> on the following topics:

- Biochemistry .. Apical Membranes
- Biochemistry .. Basolateral Membranes
- Microbiology .. Nystatin
- Physiology .. Voltage Clamp
- Physiology .. Anura
- Chemistry .. Anions

Updated information and services including high-resolution figures, can be found at:

<http://ajpcell.physiology.org/cgi/content/full/273/6/C1995>

Additional material and information about *AJP - Cell Physiology* can be found at:

<http://www.the-aps.org/publications/ajpcell>

This information is current as of November 9, 2009 .

K⁺ transport and capacitance of the basolateral membrane of the larval frog skin

STANLEY D. HILLYARD,¹ HORACIO F. CANTIELLO,² AND WILLY VAN DRIESSCHE³

¹Department of Biological Sciences, University of Nevada, Las Vegas, Nevada 89154;

²Renal Unit, Massachusetts General Hospital East and Harvard University Medical School,

Boston, Massachusetts 02129; and ³Laboratorium voor Fysiologie, Katholieke Universiteit Leuven, B-3000 Leuven, Belgium

Hillyard, Stanley D., Horacio F. Cantiello, and Willy Van Driessche. K⁺ transport and capacitance of the basolateral membrane of the larval frog skin. *Am. J. Physiol.* 273 (*Cell Physiol.* 42): C1995–C2001, 1997.—Skin from larval bullfrogs was mounted in an Ussing-type chamber in which the apical surface was bathed with a Ringer solution containing 115 mM K⁺ and the basolateral surface was bathed with a Ringer solution containing 115 mM Na⁺. Ion transport was measured as the short-circuit current (I_{sc}) with a low-noise voltage clamp, and skin resistance (R_m) was measured by applying a direct current voltage pulse. Membrane impedance was calculated by applying a voltage signal consisting of 53 sine waves to the command stage of the voltage clamp. From the ratio of the Fourier-transformed voltage and current signals, it was possible to calculate the resistance and capacitance of the apical and basolateral membranes of the epithelium (R_a and R_b , C_a and C_b , respectively). With SO_4^{2-} as the anion, R_m decreased rapidly within 5 min following the addition of 150 U/ml nystatin to the apical solution, whereas I_{sc} increased from 0.66 to 52.03 $\mu A/cm^2$ over a 60-min period. These results indicate that nystatin becomes rapidly incorporated into the apical membrane and that the increase in basolateral K⁺ permeability requires a more prolonged time course. Intermediate levels of I_{sc} were obtained by adding 50, 100, and 150 U/ml nystatin to the apical solution. This produced a progressive decrease in R_a and R_b while C_a and C_b remained constant. With Cl^- as the anion, I_{sc} values increased from 2.03 to 89.57 $\mu A/cm^2$ following treatment with 150 U/ml nystatin, whereas with gluconate as the anion I_{sc} was only increased from 0.63 to 11.64 $\mu A/cm^2$. This suggests that the increase in basolateral K⁺ permeability produced by nystatin treatment, in the presence of more permeable anions, is due to swelling of the epithelial cells of the tissue rather than the gradient for apical K⁺ entry. Finally, C_b was not different among skins exposed to Cl^- , SO_4^{2-} , or gluconate, despite the large differences in I_{sc} , nor did inhibition of I_{sc} by treatment with hyperosmotic dextrose cause significant changes in C_b . These results support the hypothesis that increases in cell volume activate K⁺ channels that are already present in the basolateral membrane of epithelial cells.

cell volume regulation; potassium channels; nystatin; epithelial transport

POTASSIUM CHANNELS in the basolateral membrane of epithelial cells allow K⁺ that is transported into the cell by the Na⁺-K⁺ pump to exit and establish a negative potential within the cell (14). Basolateral K⁺ channels are also involved in the regulation of cellular volume. For example, the basolateral membrane of turtle colon has three types of K⁺ channels, one of which is opened under conditions that promote cell swelling (5, 8, 9). The volume-sensitive K⁺ channel was also found to be blocked by lidocaine. Dawson et al. (6) subsequently

showed that substitution of a less permeant ion, gluconate, for Cl^- inhibited the lidocaine-sensitive component of the basolateral K⁺ conductance and used fluctuation analysis to demonstrate that lidocaine inhibition under swelling conditions (i.e., Cl^- as the anion) obeyed pseudo-first-order kinetics, as would be expected from a direct channel blockage.

The above studies of basolateral K⁺ permeability were conducted with epithelial tissues that were mounted in an Ussing-type chamber with K⁺ Ringer bathing the mucosal surface of the tissue and Na⁺ Ringer bathing the serosal surface. The mucosal solution also contained the ionophore amphotericin B, which formed K⁺-conducting channels in the apical membrane so that the basolateral membrane could be effectively voltage clamped and the short-circuit current (I_{sc}) could be related to the rate of basolateral K⁺ transport. We have used a similar approach to study basolateral K⁺ channels in the larval frog skin (12, 25), using the ionophore nystatin to increase apical K⁺ conductance. We have found that a period of ~1 h following nystatin treatment is required for I_{sc} to reach a maximum value. This suggests that the activation of basolateral K⁺ channels is a relatively slow process that might result from cellular swelling as K⁺ and permeant anions enter the cells across the apical membrane. Alternatively, the prolonged time course for the stimulation of I_{sc} could result from a gradual insertion of nystatin into the apical membrane. The present study was initiated to determine how quickly nystatin forms K⁺-conducting channels in the apical membrane relative to the time course for the development of maximal K⁺ transport across the basolateral membrane. Impedance analysis (24) was used to measure the resistance and capacitance of the apical and basolateral membranes (R_a and R_b , C_a and C_b , respectively) as I_{sc} increased following nystatin treatment. An increase in C_b would suggest that the increase in basolateral K⁺ transport was due to the addition of membrane vesicles, whereas lack of change in C_b would suggest that channels had become activated in situ. The larval bullfrog skin is particularly useful for this study because the limiting barrier to ion transport is a single layer of apical cells (20), the apical membrane resistance can be easily reduced by nystatin (4), and the basolateral membrane contains K⁺ channels that are activated by conditions that result in cell swelling (12).

In our studies to date, SO_4^{2-} has been used as the anion, since the basolateral membrane is highly permeable to Cl^- (11) and the low resistance of the tissue complicates fluctuation analysis measurements. We

have found that quinine, quinidine, lidocaine (26), and more recently verapamil (12) inhibit that fraction of the I_{sc} that can also be inhibited by treatment with hyperosmotic sucrose solutions. A second goal of the study was to determine whether substitution of anions that are progressively less permeant (i.e., Cl⁻, SO₄²⁻, and gluconate) or the addition of hypersomotic solute concentrations results in a lower stimulation of basolateral K⁺ conductance and to measure R_b and C_b under these conditions. If the stimulation of basolateral K⁺ transport is the result of cell swelling due to the entry of more permeant anions, there should be a progressive decrease in I_{sc} and increase in R_b with the less permeant anions or the addition of an impermeant solute. If these changes in I_{sc} and R_b are the result of removal of membrane vesicles, C_b would be predicted to decrease in proportion to the decrease in I_{sc} .

METHODS

Larval bullfrogs, *Rana catesbeiana*, were obtained from commercial suppliers and maintained in aquaria at 15°C. The ventral skin was dissected with the abdominal musculature attached (4), using MS 222 anesthesia. The skin was mounted in an Ussing-type chamber that minimized edge damage and permitted continuous perfusion of the mucosal and serosal solutions (7). The mucosal solution contained 115 mM K⁺ and 1.0 mM Ca²⁺, with either Cl⁻, SO₄²⁻, or gluconate as the anion, and 2.5 mM KHCO₃. The serosal solution contained 115 mM Na⁺ and 1.0 mM Ca²⁺, with either Cl⁻, SO₄²⁻, or gluconate as the anion, and 2.5 mM KHCO₃. The pH of both solutions was 8.0. Once stable values for I_{sc} had been obtained, nystatin (Sigma Chemical) was added to the mucosal Ringer to give the desired concentration. The appropriate amount of nystatin was dissolved in 100 μl dimethyl sulfoxide per 100 ml Ringer.

The macroscopic I_{sc} was applied with a low-noise voltage clamp and was recorded on a chart recorder. The direct current (DC) resistance of the entire tissue (R_m) was measured by applying a 10-mV pulse to the command stage of the voltage clamp and dividing by the change in I_{sc} . For impedance measurements, the command stage of the voltage clamp was connected to a computerized voltage signal composed of 53 sine waves, and the voltage and current signals from the clamp were sampled consecutively. The voltage and current signals were subjected to a fast Fourier transform, and the impedance (Z) was calculated as the ratio of the transformed voltage and current signals (see Refs. 16 and 22 for detailed description of the synchronization of the voltage and current signals). Two impedance curves were merged and plotted as impedance loci on Nyquist plots. Before nystatin treatment, the Nyquist plots contained a single semicircle. This semicircle could be fitted with Eq. 1, which assumes a single membrane with parallel resistance (R) and capacitance (C) elements (Ref. 24, adapted from Ref. 3)

$$Z(f) = \frac{R}{1 + (j\omega RC)^\alpha} \quad (1)$$

In this equation, $j = \sqrt{-1}$ and ω is the angular frequency = $2\pi f$, where f is frequency. The exponent $\alpha = 1 - 2\phi/\pi$, where ϕ is the angle, in degrees, between the line that connects the center of the semicircle with its intercept on the real (resistance) axis. This equation provides an accurate measurement of tissue capacitance (C_m) that is equivalent to C_a before nystatin treatment, since the apical membrane is the domi-

nant resistance element (24). It should be noted, however, that the resistance elements calculated by Eq. 1 include that of R_a and R_b in series and the paracellular pathway (R_p) that is in parallel with R_a and R_b . Thus the resistance calculated by Eq. 1, before the addition of nystatin, should be equal to R_m and, since the R_a is very high, should provide an approximate measure of R_p .

After nystatin treatment, two semicircles frequently appeared in the Nyquist plots. To fit the two semicircles, Eq. 1 can be used separately for each (24), and the resistance values calculated by this equation approximate R_a and R_b . Alternatively, Margineanu and Van Driessche (17) developed an expression for transepithelial impedance [$Z(t)$] that fits two semicircles, with the assumption that they represent two membranes in series, each with a parallel resistance and capacitance (e.g., R_a , R_b , C_a , C_b). This model also incorporates an expression for the paracellular shunt resistance (R_p) that is in parallel with the apical and basolateral membranes

$$Z(t) = Rs + \frac{As^\alpha + B}{Cs^{2\alpha} + Ds^\alpha + 1} \quad (2)$$

In Eq. 2, s is the product $j\omega$, and A, B, C, and D contain terms that relate to R_p , R_a , R_b , C_a , and C_b

$$A = R_p[R_a(R_b C_b) + R_b(R_a C_a)]/N$$

$$B = R_p(R_a + R_b)/N$$

$$C = R_p(R_a C_a R_b C_b)/N$$

$$D = [R_b(R_a C_a) + R_a(R_b C_b) + R_p[(R_a C_a) + (R_b C_b)]]/N$$

$$N = R_a + R_b + R_p$$

A, B, C, and D were obtained by nonlinear curve fitting of Eq. 2 to the impedance data as described by Margineanu and Van Driessche (17). Values for R_p were taken to be the resistance values (R_m) calculated from the DC voltage pulses before nystatin treatment. As indicated above, the apical membrane of the larval skin has a very high DC resistance (4), and it was assumed that the resistance of the skin with an intact apical membrane approximates R_p .

To follow the time course of impedance changes as I_{sc} was stimulated, Nyquist plots were generated at 5-min intervals for 60 min following the addition of nystatin at a concentration of 150 U/ml, which we have found to produce maximal I_{sc} values (25). In a second series of experiments, I_{sc} was more gradually stimulated by sequentially adding 50, 100, and 150 U/ml nystatin. Impedance was determined when I_{sc} had reached stable values at each concentration. The above experiments were conducted with SO₄²⁻ as the anion.

The effect of different anions was assessed by conducting separate sets of experiments using Cl⁻, SO₄²⁻, or gluconate as the anion. Skins were treated with 150 U/ml nystatin, and impedance was determined after stable I_{sc} values had been achieved.

Finally, the effect of increasing the osmotic concentration was evaluated by adding dextrose, in concentrations between 10 and 50 mM, to the mucosal and serosal solutions of preparations having SO₄²⁻ as the anion. Dextrose was added after I_{sc} had equilibrated following mucosal treatment with 150 U/ml nystatin.

Statistical comparisons between current, resistance, and capacitance values were made with Student's t -test.

RESULTS

The time course for the stimulation of I_{sc} by the addition of nystatin to the mucosal Ringer is shown in

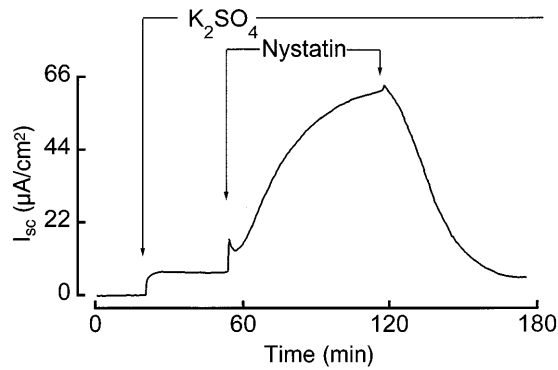


Fig. 1. Tracing of short-circuit current (I_{sc}) recorded when K_2SO_4 Ringer replaced Na_2SO_4 Ringer as mucosal solution and when 150 U/ml nystatin was subsequently added to mucosal solution. Note also that I_{sc} returns toward control levels when nystatin is removed from mucosal solution.

Fig. 1. Note the immediate rise in I_{sc} followed by a slower but larger increase in I_{sc} over a 1-h period. Note also that the nystatin effect could be reversed after removal from the mucosal Ringer. Nyquist plots obtained before nystatin treatment and after stimulation of I_{sc} with 150 U/ml nystatin are shown in Fig. 2. The magnitudes of the resistive and capacitive components of the plot obtained after nystatin treatment were multiplied by a scale factor of five to illustrate the presence of a second semicircle, and the points were fitted by Eq. 2. The plot obtained before nystatin treatment was fitted with Eq. 1.

R_m decreased to minimal values within 5 min following nystatin treatment. It was found that resistance values calculated from the fit of the pretreatment plots by Eq. 1 were almost identical with R_m (Fig. 3A). After nystatin treatment, the fit with Eq. 2 showed that the smaller semicircle nearer the origin of the Nyquist plot (the higher-frequency impedance loci) represented the apical membrane, since C_a values were the same as those seen before nystatin treatment (see below) and R_a values declined in parallel with R_m as would be expected when nystatin formed channels in the apical membrane. The larger semicircle represented the baso-

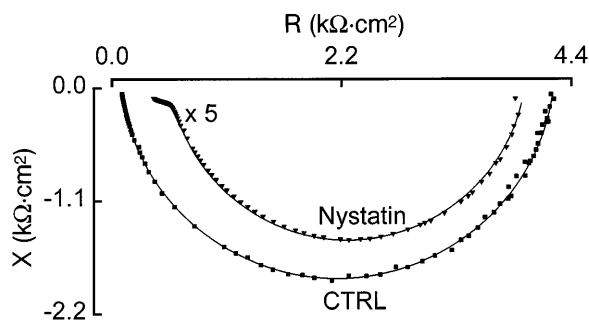


Fig. 2. Nyquist plots obtained before nystatin treatment [control (CTRL)] and after maximal I_{sc} values were obtained following nystatin treatment. Control plot was fitted with Eq. 1, and plot obtained after nystatin treatment was fitted with Eq. 2. Plot obtained after nystatin treatment was amplified by a scaling factor of 5 to illustrate presence of 2nd semicircle that represents apical membrane. R , resistance; X , capacitance.

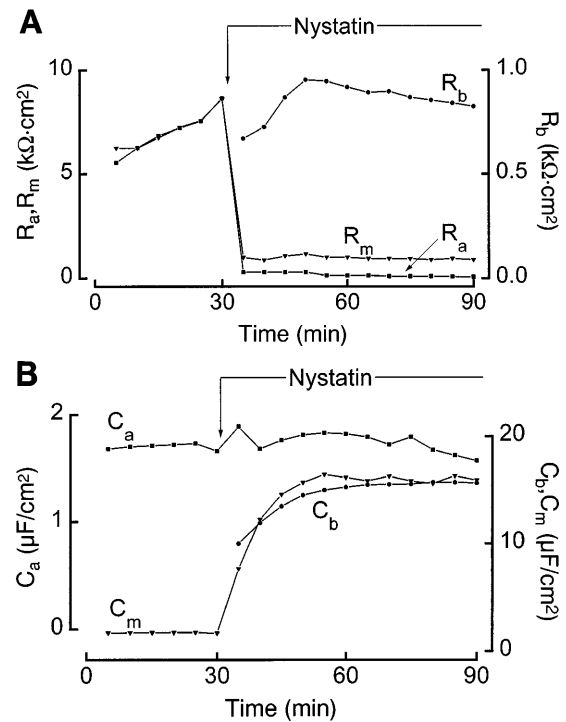


Fig. 3. *A*: changes in apical, basolateral, and skin resistance (R_a , R_b , and R_m , respectively) produced by addition of 150 U/ml nystatin to mucosal Ringer (at time indicated by arrow at top). See text for description of methods used to determine these terms. *B*: changes in apical, basolateral, and tissue capacitance (C_a , C_b , and C_m , respectively) that were calculated from same Nyquist plots used to measure R_a and R_b in *A*. C_m was calculated from fit of larger semicircle of Nyquist plot with Eq. 1. Arrow, time of nystatin addition.

lateral membrane, which constitutes most of the resistance (R_b) following 150 U/ml nystatin treatment.

Apical capacitance was calculated from Eq. 1 before nystatin treatment and by Eq. 2 following nystatin treatment (Fig. 3B). The two fits gave values for apical capacitance that were not significantly different. The presence of the second semicircle following nystatin treatment allowed the calculation of C_b by Eq. 2. It was also possible to use Eq. 1 to fit the larger semicircle during the time course of nystatin treatment and obtain a measure of C_m when the basolateral membrane was the primary resistance element of the tissue. To demonstrate that the single and double fits gave similar values for basolateral membrane capacitance, a series of 22 preparations was evaluated after I_{sc} had equilibrated with 150 U/ml nystatin in the mucosal Ringer. The values for C_b were 12.73 ± 0.77 and $13.41 \pm 0.74 \mu F/cm^2$ with Eqs. 1 and 2, respectively, and were not significantly different.

Both C_m and C_b increased during the first 15 min following nystatin treatment as the basolateral membrane became the major component of the Nyquist plot. Also, I_{sc} was rapidly increasing during this period as the cells responded to the rapid increase in K^+ entry across the apical membrane. Given the sampling time required to obtain values at the lower frequencies (~ 150 s), it was desirable to measure resistance and capacitance at stable values of I_{sc} that were intermedi-

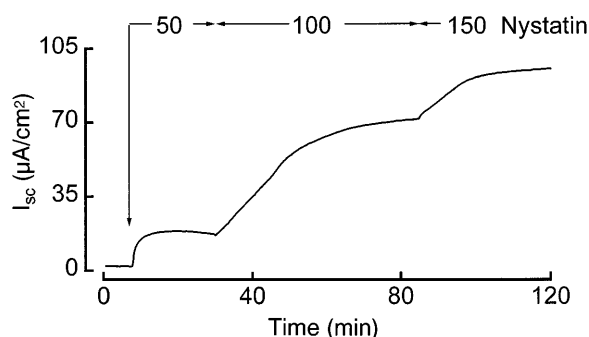


Fig. 4. A tracing of I_{sc} obtained when nystatin concentration of mucosal solution was raised incrementally from 50 to 100 to 150 U/ml. Nyquist plots were obtained when I_{sc} had stabilized at each concentration.

ate between pretreatment and maximal values. This was accomplished by exposing the apical membrane to intermediate concentrations of nystatin. It can be seen in Fig. 4 that sequential treatment with 50, 100, and 150 U/ml nystatin in the mucosal Ringer produced progressively higher I_{sc} values that were stable throughout the sampling period required for impedance measurements. Mean values for the stable I_{sc} and R_m values for five such preparations are given in Table 1. Impedance measurements at these intermediate I_{sc} values showed the appearance of a second semicircle that became the dominant component at the highest nystatin concentration (Fig. 5). Results from 13 preparations showed that R_a decreased to a small fraction of the tissue resistance; however, C_a remained relatively constant (Table 2). The decrease in R_a with increasing nystatin concentrations corresponds to the increase in I_{sc} and a decrease in R_b . The values for C_b , however, were not found to be significantly different.

When the Ringer solutions contained Cl⁻ as the anion, the I_{sc} values obtained after treatment with 150 U/ml nystatin were greater and R_b was lower than those observed with SO₄²⁻ (Fig. 6). In contrast, lower values for I_{sc} and higher values for R_b were noted when gluconate was substituted for SO₄²⁻. Values for C_b obtained with the three anions were not significantly different, despite the large differences in I_{sc} and R_b . We also observed, as seen with SO₄²⁻ in Fig. 3B, that the elevation of C_b recorded during the first 10–20 min following the addition of 150 U/ml nystatin was seen regardless of the anion and the resulting degree to which I_{sc} was stimulated (not shown).

Table 1. I_{sc} and R_m after serial addition of nystatin

	I_{sc} , $\mu\text{A}/\text{cm}^2$	R_m , $\Omega \cdot \text{cm}^2$
Control	1.29 ± 0.07	11,111 ± 1,235
50 U/ml nystatin	10.52 ± 2.24	4,167 ± 868
100 U/ml nystatin	36.08 ± 9.99	1,563 ± 415
150 U/ml nystatin	65.4 ± 8.21	555 ± 126

Values are means ± SE of 5 preparations for short-circuit current (I_{sc}) and skin resistance (R_m ; calculated from direct current pulses) after serial addition of 50, 100, and 150 U/ml nystatin in preparations with SO₄²⁻ as anion.

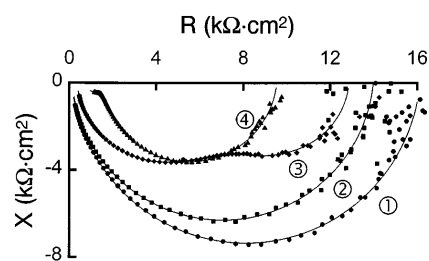


Fig. 5. Nyquist plots obtained before nystatin treatment (control) of mucosal Ringer (curve 1; ●) and under conditions of stable I_{sc} following treatment with 50 (curve 2; ■), 100 (curve 3; ◆), and 150 (curve 4; ▲) U/ml nystatin. Scales of Nyquist plots obtained after treatment with 100 and 150 U/ml nystatin were multiplied by a factor of 5 to better illustrate emergence of semicircle that represents basolateral membrane.

The addition of dextrose produced a dose-dependent inhibition of I_{sc} in conjunction with an increase in R_m (Fig. 7). The values for C_m (fitted with Eq. 1) that were obtained when stable I_{sc} values were obtained at each dextrose concentration were not significantly different from that obtained before dextrose treatment.

DISCUSSION

The decrease in tissue resistance (R_m or by Eq. 1 or Eq. 2) within 5 min after the addition of 150 U/ml nystatin to the mucosal Ringer shows that nystatin inserts rapidly into the apical membrane. It is also evident from Fig. 1 that nystatin washes out of the apical membrane when removed from the mucosal Ringer. The development of maximal I_{sc} values during the 1 h following treatment with the highest nystatin concentration is thus the result of a more prolonged time course for the stimulation of basolateral K⁺ permeability. After the initial decline in R_a , R_m values were essentially identical with R_b but did not decrease further, despite the continued increase in I_{sc} . This could be a result of other ions becoming permeable across the basolateral membrane as R_a became maximally reduced or possibly is a result of the increasing I_{sc} interfering with the impedance measurements.

In contrast, when the nystatin concentration was increased incrementally, R_b did decrease as I_{sc} values

Table 2. Impedance parameters calculated for skins treated with 0, 50, 100, and 150 U/ml nystatin

	R_a , $\Omega \cdot \text{cm}^2$	C_a , $\mu\text{F}/\text{cm}^2$	R_b , $\Omega \cdot \text{cm}^2$	C_b , $\mu\text{F}/\text{cm}^2$
Control	12,079 ± 1,630	1.61 ± 0.03		
50 U/ml nystatin	2,386 ± 361	1.78 ± 0.08	4,249 ± 851	17.1 ± 1.1
100 U/ml nystatin	226 ± 64	1.79 ± 0.19	1,820 ± 337	14.3 ± 0.08
150 U/ml nystatin	80 ± 6.8	1.43 ± 0.08	549 ± 34	15.1 ± 0.9

Values are means ± SE of 13 preparations. As noted in text, control values for resistance that were measured before nystatin treatment were obtained with Eq. 1, in which total tissue resistance is measured and the dominant resistance element across skin is assumed to be paracellular pathway resistance (R_p). Resistance and capacitance values following nystatin treatment were calculated with Eq. 2. R_a , apical resistance; R_b , basolateral resistance; C_a , apical capacitance; C_b , basolateral capacitance.

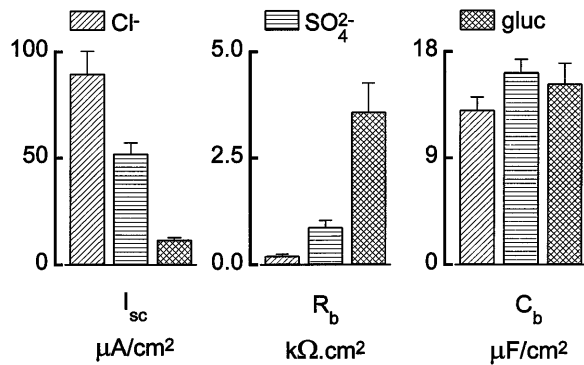


Fig. 6. Effect of substituting more permeant cations [$\text{Cl}^- > \text{SO}_4^{2-} > \text{gluconate (gluc)}$] on I_{sc} (left), R_b (middle), and C_b (right) in preparations treated with 150 U/ml nystatin in mucosal Ringer. R_b and C_b were calculated from fits of Nyquist plots with Eq. 2.

increased when R_a was lowered by the ionophore, suggesting that K^+ permeability was a major component of basolateral resistance under these conditions. In either case, an increase in the entry of K^+ into the cells was compensated for by an increase in K^+ permeability across the basolateral membrane. It is unlikely, however, that the K^+ gradient per se is the determining factor for the reduction of R_b , since the increase in I_{sc} ($\text{Cl}^- > \text{SO}_4^{2-} > \text{gluconate}$) and decrease in R_b ($\text{Cl}^- < \text{SO}_4^{2-} < \text{gluconate}$) that were observed with anion substitution occurred with the highest nystatin concentration and with comparable gradients for K^+ transport across the tissue. Gluconate substitution for Cl^- is known to reduce cellular swelling in turtle colon cells after treatment with amphotericin B (6). The increase in basolateral K^+ permeability of the larval frog skin bathed either with more permeant anions or with increasing nystatin concentrations is probably regulated as part of a volume regulatory decrease, as is the

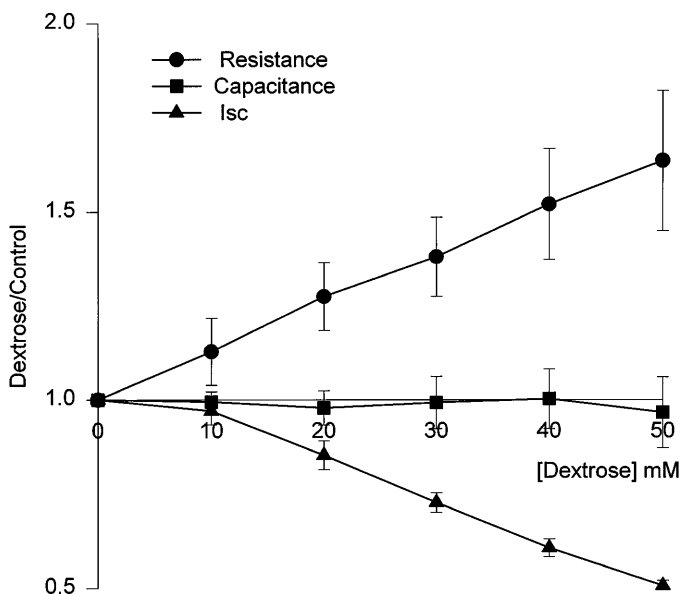


Fig. 7. Adding dextrose to mucosal and serosal Ringer in preparations having SO_4^{2-} as anion and 150 U/ml nystatin in mucosal solution causes a decrease in I_{sc} (▲) and an increase in R_m (●) but no change in C_b (■). C_b was calculated with Eq. 1.

case for most cells faced with conditions that promote swelling (15, 25). The reduction of I_{sc} and the increase in R_m that accompanied the addition of dextrose to the bathing solutions further support the hypothesis that the cells are responding to the osmotic rather than an ionic effect of anion substitution.

There was an apparent increase in C_b and C_m during the 15 min following the addition of 150 U/ml nystatin. This occurred during the transition from the pretreatment conditions, in which the apical membrane is the dominant component of the Nyquist plots, to the equilibrium condition, in which the basolateral membrane is the major component and I_{sc} values are increasing rapidly. The collection of impedance data requires that two curves be generated with fundamental frequencies of 3.2 and 0.5 Hz (17). Multiple sweeps are taken for each record, so that a total of ~ 150 s is needed for data acquisition. Changes in I_{sc} that result from increasing K^+ conductance across the membrane during this sampling interval could result in errors in measurement of capacitance. This transient increase in C_b was comparably seen in experiments with all three anions, even though the increase in I_{sc} was markedly different among gluconate, SO_4^{2-} , and Cl^- . Thus, if the increase in capacitance represents an addition of membrane vesicles to the basolateral membrane, it does not appear to be associated with the magnitude of the increase in K^+ permeability. In contrast, C_b values that were calculated after stable I_{sc} values had been obtained, either from preparations treated with 150 U/ml nystatin or with stepwise addition of 50, 100, and 150 U/ml nystatin, were not different, even though R_b was lowered by a factor of eight. Values for C_b that were calculated from either Eq. 1 or Eq. 2 were not significantly different, and the value for R_p chosen for Eq. 2 was assumed not to change as R_b decreased. The similar values for C_b obtained by both calculations suggest that changes in R_p , if they occur, are small.

That C_b was not different despite large changes in R_b and I_{sc} provides evidence that the activation of basolateral K^+ channels does not require the net addition of vesicles to the basolateral membrane and that channels are activated in situ by cell swelling. These results are consistent with observations by Cantiello et al. (2) that activation of volume-sensitive K^+ channels in melanoma cells is dependent on actin-binding protein and their suggestion that volume activation of channels involves an interaction between the actin cytoskeleton and volume-sensitive channels in the membrane.

As noted above, there was a transient increase in C_b as I_{sc} values increased in the first 15 min following the addition of 150 U/ml nystatin in experiments with all three anions. If this does, in fact, represent the addition of basolateral vesicles (as opposed to being the result of increasing I_{sc} values during data acquisition), it could be that insertion of new K^+ channels is taking place but the activation of these channels requires the volume change associated with the more permeant anions. Experiments to date have shown that blocker-sensitive channels (i.e., verapamil, quinidine, quinine) are also inhibited by the addition of hyperosmotic sugar solu-

tions (12) or gluconate as the anion (unpublished observations). In these experiments, a two-state model for blocker-induced noise analysis has been used, and measurements of open probability are not available. Furthermore, comparison of the kinetics of blocker action on current fluctuations and on the inhibition of I_{sc} indicates that the kinetics of basolateral K⁺ channels in larval frog skin and in turtle colon (6, 12) are complex, so that the specific mechanism of channel activation remains elusive.

The lack of change in C_b does not completely rule out the possibility that membrane retrieval and insertion are occurring at comparable rates so that new channels are added as membrane vesicles with a lower channel density are retrieved. Increases in membrane capacitance have been shown to correlate with the addition of water-conducting aggregophores in the amphibian urinary bladder (13, 19, 22), and it has been suggested that the stimulation of apical membrane Na⁺ conductance of A6 cells by antidiuretic hormone is associated with the addition of membrane vesicles containing amiloride-sensitive Na⁺ channels (18). Harris et al. (10) found that conditions that favor cellular swelling result in greater rates of exocytosis and endocytosis of apical membrane vesicles by toad urinary bladder granular cells when osmotic water flux is stimulated by antidiuretic hormone.

Using noise analysis, Van Driessche and Hillyard (25) estimated the density of basolateral K⁺ channels in the larval frog skin to be 7.7 channels/ μm^2 of cross-sectional area. Because the capacitance measurements used to estimate the basolateral membrane area suggest that the actual basolateral membrane area is ~10- to 15-fold greater than the cross-sectional area, the density of channels would be on the order of 0.5–1 μm^{-2} . Thus a small turnover of vesicles having a high density of channels could result in substantial changes in K⁺ transport as the channels became activated.

Another caveat in the interpretation of the capacitance values is the possibility that the dielectric behavior of cell membranes in this tissue is frequency dependent, so that capacitance values obtained over a range of frequencies would give rise to errors in capacitance measurements (1). With Eqs. 1 and 2, membrane resistance and capacitance values are determined over the same range of frequencies, and the resistance values, R_a and R_b , are very similar to the values for R_m that were obtained with a single DC voltage pulse. Even with errors in the determination of absolute values for C_b , the lack of observed differences in this parameter over the wide range of resistances and I_{sc} values produced in the experimental treatments is most consistent with the activation of in situ channels and/or a very precise mechanism for the control of basolateral membrane area.

We gratefully acknowledge the technical assistance of J. De Beir Simaels.

S. D. Hillyard was supported in part by National Science Foundation Grant IBN-9215023 and National Institute of Diabetes and Digestive and Kidney Diseases Grant DK-38977-01. H. F. Cantiello was supported in part by National Institute of Diabetes and Digestive

and Kidney Diseases Grant DK-48040, and W. Van Driessche was supported by Grant G.023.95 from the Fonds Wetenschappelijk-Vlaanderen (Belgium).

Address for reprint requests: S. D. Hillyard, Dept. of Biological Sciences, University of Nevada, 4505 Maryland Pkwy., Las Vegas, NV 89154-4004.

Received 30 September 1996; accepted in final form 21 August 1997.

REFERENCES

1. **Aywada, M., and S. I. Helman.** Na⁺ transport related changes of apical membrane capacitance in the tight epithelium of frog skin (Abstract). *FASEB J.* 6: A1239, 1992.
2. **Cantiello, H. F., A. G. Prat, J. V. Bonventure, C. C. Cunningham, J. H. Hartwig, and D. A. Ausiello.** Actin-binding protein contributes to cell volume regulatory ion channel activation in melanoma cells. *J. Biol. Chem.* 268: 4596–4599, 1993.
3. **Cole, K. S., and R. H. Cole.** Dispersion and absorption in dielectrics. I. Alternating current characteristics. *J. Chem. Phys.* 9: 341–351, 1940.
4. **Cox, T. C., and R. H. Alvarado.** Electrical and transport characteristics of skin of larval *Rana catesbeiana*. *Am. J. Physiol.* 237 (Regulatory Integrative Comp. Physiol. 6): R74–R79, 1979.
5. **Dawson, D. C., and N. W. Richards.** Basolateral K conductance: role in regulation of NaCl absorption and secretion. *Am. J. Physiol.* 259 (Cell Physiol. 28): C181–C195, 1990.
6. **Dawson, D. C., W. Van Driessche, and S. I. Helman.** Osmotically induced basolateral K⁺ conductance in turtle colon: lidocaine-induced K⁺ channel noise. *Am. J. Physiol.* 254 (Cell Physiol. 23): C165–C174, 1988.
7. **De Wolf, I., and W. Van Driessche.** Voltage-dependent Ba²⁺ block of K⁺ channels in the apical membrane of frog skin. *Am. J. Physiol.* 251 (Cell Physiol. 20): C696–C706, 1986.
8. **Germann, W. J., S. A. Ernst, and D. C. Dawson.** Resting and osmotically-induced basolateral K conductances in turtle colon. *J. Gen. Physiol.* 88: 253–274, 1986.
9. **Germann, W. J., M. E. Lowy, S. A. Ernst, and D. C. Dawson.** Differentiation of two distinct K conductances in the basolateral membrane of turtle colon. *J. Gen. Physiol.* 88: 237–252, 1986.
10. **Harris, H. W., J. B. Wade, and J. S. Handler.** Fluorescent markers to study membrane retrieval in antidiuretic hormone-treated urinary bladder. *Am. J. Physiol.* 251 (Cell Physiol. 20): C274–C284, 1986.
11. **Hillyard, S. D.** Osmotically regulated Cl⁻ conductance across the basolateral membrane of the tadpole skin epithelium (Abstract). *Physiologist* 30: 156, 1987.
12. **Hillyard, S. D., and W. Van Driessche.** Verapamil blocks basolateral K⁺ channels in the larval frog skin. *Am. J. Physiol.* 262 (Cell Physiol. 31): C1161–C1166, 1992.
13. **Kachadorian, W. A., J. B. Wade, and V. A. DiScala.** Vasopressin-induced structural change in toad bladder luminal membrane. *Science* 190: 67–69, 1975.
14. **Koefoed-Johnsen, V., and H. H. Ussing.** The nature of the frog skin potential. *Acta Physiol. Scand.* 42: 298–308, 1958.
15. **Lewis, S. A., and P. Donaldson.** Ion channels and cell volume: chaos in an organized system. *News Physiol. Sci.* 5: 112–119, 1990.
16. **Lindemann, B., and W. Van Driessche.** Sodium-specific membrane channels of frog skin are pores: current fluctuations reveal high turnover. *Science* 195: 292–294, 1977.
17. **Margineanu, D.-G., and W. Van Driessche.** Effects of millimolar concentrations of glutaraldehyde on the electrical properties of frog skin. *J. Physiol. (Lond.)* 427: 567–581, 1990.
18. **Marunaka, Y., and D. C. Eaton.** Effects of vasopressin and cAMP on single amiloride-blockable channels. *Am. J. Physiol.* 260 (Cell Physiol. 29): C1071–C1084, 1991.
19. **Palmer, L. G., and M. Lorenzen.** Antidiuretic hormone-dependent membrane capacitance and water permeability in the toad urinary bladder. *Am. J. Physiol.* 244 (Renal Fluid Electrolyte Physiol. 13): F195–F204, 1983.
20. **Robinson, D. A., and M. B. Heintzelman.** Morphology of the ventral epidermis of *Rana catesbeiana* during metamorphosis. *Anat. Rec.* 217: 305–317, 1987.

21. **Schultz, S. G.** Volume preservation then and now. *News Physiol. Sci.* 4: 169–171, 1989.
22. **Stetson, D. L., S. A. Lewis, W. Alles, and J. B. Wade.** Evaluation by capacitance measurements of antidiuretic hormone-induced membrane area changes in toad bladder. *Biochim. Biophys. Acta* 689: 267–274, 1982.
23. **Van Driessche, W.** Noise and impedance analysis. In: *Methods in Membrane and Transporter Research*, edited by J. A. Schafer, G. Giebisch, P. Kristensen, and H. H. Ussing. Austin, TX: Landes, 1994.
24. **Van Driessche, W.** Lidocaine blockade of basolateral potassium channels in the amphibian urinary bladder. *J. Physiol. (Lond.)* 381: 575–593, 1986.
25. **Van Driessche, W., and S. D. Hillyard.** Quinidine blockage of K⁺ channels in the basolateral membrane of larval bullfrog skin. *Pflügers Archiv* 405, *Suppl.* 1: S77–S82, 1985.
26. **Van Driessche, W., S. D. Hillyard, and H. Cantiello.** Investigations of basolateral K⁺ channels of the tadpole skin epithelium with noise analysis (Abstract). *Federation Proc.* 44: 1567, 1985.

